Journal of Manufacturing and Materials Processing

MDPI

Article

Removing High-Velocity Oxyfuel Coatings Through Electrolytic Dissolution

Zdeněk Pitrmuc [1], Vivek Rana [1], Michal Slaný [1], Jiří Kyncl [1], Sunil Pathak [1,2,*] and Libor Beránek [1]

[1] Department of Machining, Process Planning and Metrology, Faculty of Mechanical Engineering, Czech Technical University in Prague, 160 00 Prague, Czech Republic; zdenek.pitrmuc@fs.cvut.cz (Z.P.); vivek.rana@fs.cvut.cz (V.R.); michal.slany@fs.cvut.cz (M.S.); jiri.kyncl@cvut.cz (J.K.); libor.beranek@fs.cvut.cz (L.B.)

[2] HiLASE Centre, Institute of Physics of Czech Academy of Sciences, 182 00 Prague, Czech Republic

* Correspondence: sunilpathak87@gmail.com or sunil.pathak@hilase.cz or sunil.pathak@fs.cvut.cz

Abstract: High-velocity oxyfuel (HVOF) coatings are used to protect components from corrosion and wear at higher temperatures and from wearing out after a certain period of time. Hence, to enhance the life of components, further recoating is required, but removing the older coating is a challenging task due to its high hardness. Thus, this research work studied the electrolytic dissolution process of removing WC-CoCr 86/10/4 HVOF coatings and found that at a voltage of 3 V, the coating was not removed, but at a slightly higher voltage of 6 V, the coating was removed completely. When the voltage was 12 V, the surface was damaged, and corrosion also occurred. A combination of tartaric acid ($C_4H_6O_6$), sodium bicarbonate ($NaHCO_3$), and water was used as an electrolyte. By using a combination of a voltage of 4.5 V, a current of 1.6 A, and an electrode distance of 55 mm, the coating was completely removed after 10 h, with negligible attacks on the base material. Where the corrosion of the base material is unacceptable, voltages in the range of 4 to 6 V are recommended. If parts have coatings on all surfaces, a voltage within the range of 6 to 12 V can be recommended. The coating from tab SB-002JI-5 TOOLOX-11 and hexagonal mandrel SB-00EA-1 160 TIS was also removed successfully.

Keywords: HVOF coatings; electrolytic dissolution; coating removal; current density

Academic Editor: Steven Y. Liang

Received: 19 December 2024
Revised: 24 January 2025
Accepted: 25 January 2025
Published: 29 January 2025

Citation: Pitrmuc, Z.; Rana, V.; Slaný, M.; Kyncl, J.; Pathak, S.; Beránek, L. Removing High-Velocity Oxyfuel Coatings Through Electrolytic Dissolution. *J. Manuf. Mater. Process.* **2025**, *9*, 40. https://doi.org/10.3390/jmmp9020040

1. Introduction

Hard coatings are used to prevent components from corrosion, wear, and hydrogen embrittlement, and they have higher fatigue strength, hence improving their service life [1,2]. HVOF coatings, among the different types of hard coatings, provide very high adhesion and dense structure; hence, they are very difficult to remove. HVOF coatings show high wear resistance [3], and they are used in tribological [4], maritime [5,6], and aviation applications [7–9]; earth moving equipment [10]; and automobiles [11].

The coating removal process is of great importance for industries involved in the repair and overhaul of components. These coatings, such as WC-Co coatings, have microhardness values in the range of 1200–1300 kg/mm^2 (Knoop hardness) [12]. Nahvi et al. [13] investigated different WC-based coatings, measuring their microhardness, porosity, and fracture toughness. The investigated cermets were WC-Co, WC-FeCrAl, and WC-Ni-MoCrFeCo, with hardness values of 1305 ± 71 $HV_{0.3}$, 1498 ± 82 $HV_{0.3}$, and 1254 ± 38 $HV_{0.3}$, respectively. Thus, HVOF coatings have very high hardness and can be difficult to remove via machining processes or other means. Sahraoui et al. [14] used HVOF coatings to

replace chromium coatings for repairing gas turbine shafts and found them to be better alternatives with high hardness and wear resistance. The most severe degradation modes that gas turbine shafts have to face are friction and wear. The surface damage generated by the sliding contact with bearings limits the life of the shafts and therefore reduces their durability and reliability. Electroplating for repairing the components takes more time compared to HVOF coatings, and it is also inferior in mechanical properties [15,16]. Ruusuvuori et al. [17] used an Abrasive Water Jet (AWJ) to remove WC-CoCr and Cr_3C_2-NiCr HVOF coatings using Al_2O_3 abrasives and reduced the coating thickness to 10–20 μm. However, this process may damage the base material. In general, HVOF hard metal coating thicknesses range between 50 and 450 μm [18,19]. The coating removal method should have the following aspects: (i) retain substrate integrity, (ii) exhibit a high removal rate, (iii) lead to uniform dissolution, (iv) show no galvanic corrosion, and (v) be environmentally friendly. For economical recoating, an efficient coating removal method is required.

The effective removal of HVOF coatings is limited by existing methods. This research focuses on electrolytic dissolution as a potential solution. In this process, the material is removed by an atom/molecule, and this is a non-contact-type process; hence, the integrity of the base material is not damaged in comparison with other contact-type processes. However, this process has limitations, and it can be used only for conductive materials. This process requires an electrolyte and an extended time period, which can be highly corrosive in nature; hence, this process's apparatus has high costs, and extra care during handling is required. Experiments were conducted to study the effects of voltage, surface area, electrode distance, and electrolyte temperature on current density and coating removal. The HVOF coating was also removed from real applications to verify the capability of the electrolytic dissolution process.

2. Materials and Methods

In this section, the details of the sample preparation, electrolyte selection, and experimental planning are discussed.

2.1. Sample Preparation

Eight samples made of tool steel Toolox 44 (chemical composition in wt%: 0.32% C; 0.8% Mn; 0.6% Si; 1.35% Cr; 0.8% Mo; 0.14% V; 0.7% Ni; and remaining Fe [20]) were chosen at a size of 20 × 10 × 100 mm, and an HVOF coating was provided for the surface, with dimensions of 20 × 100 mm. The samples were marked on the side with numbers for easy discernability, as shown in Figure 1. These samples were further cut into a size of 20 × 10 × 10 mm for studying the initial state of the coating, and thicknesses were in the range of 0.3–0.4 mm, as shown in Figure 1b.

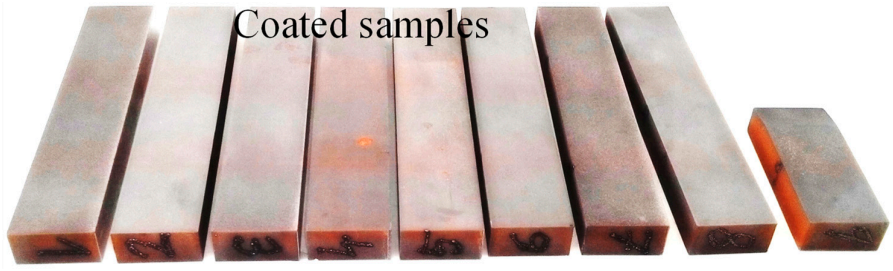

(**a**)

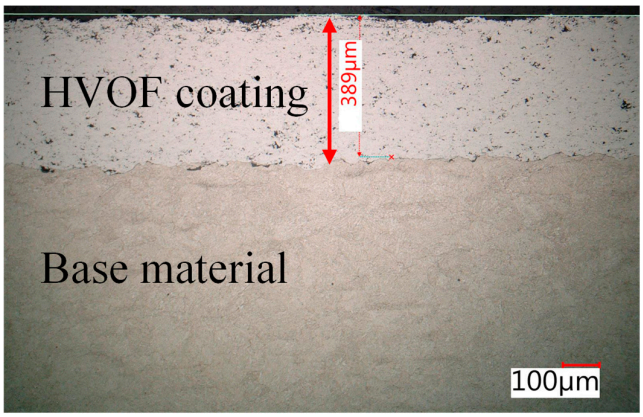

(**b**)

Figure 1. Samples: (**a**) with HVOF coating; (**b**) cross-sectional view.

2.2. Electrolyte Selection

Two stripped electrodes were dipped in the electrolyte bath as shown in Figure 2a. The coated sample was connected to the positive terminal of the direct current (DC) voltage and known as an anode, whereas the other electrode was connected to the negative terminal of the DC voltage and known as a cathode. The electrolyte chamber was made of an acrylic sheet, which is a non-conductive, non-corrosive, and dimensionally stable material. The electrolyte is the important factor in this process for HVOF coating removal.

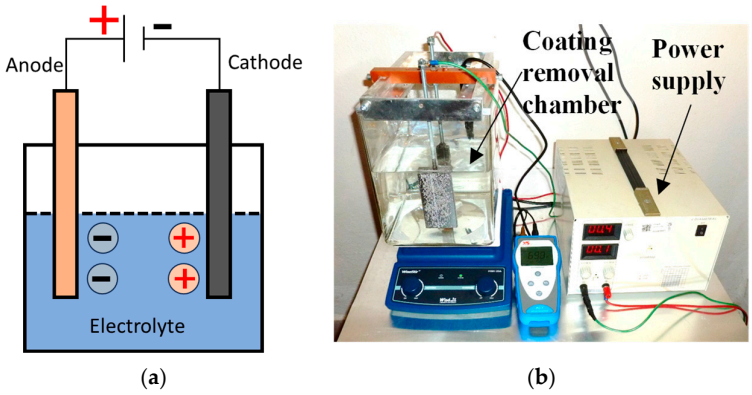

(**a**) (**b**)

Figure 2. Test equipment: (**a**) schematic and (**b**) developed equipment.

Before selecting the appropriate electrolyte, the experiments were performed with three different electrolytes, i.e., (i) HCl + HF + ethanol, (ii) Struers A2 electrolyte containing perchloric acid ($HClO_4$) and a mixture of alcohols, and (iii) tartaric acid ($C_4H_6O_6$) + sodium bicarbonate ($NaHCO_3$) + water (H_2O).

The electrolyte containing hydrochloric acid (HCL) and hydrofluoric acid (HF) preferentially attacked the base material of the steel, and without its masking, the coating would not be practically removed. In addition, the removal was not uniform and point etching occurred. The handling and disposal of this electrolyte entails significant safety and environmental risks.

The commercially available Struers A2 electrolyte contains perchloric acid ($HClO_4$) and a mixture of alcohols. It removed the coating, but it smoothly transitioned into corrosion of the base material. Perchloric acid represents an ecological burden, and safety precautions must be taken during its handling and disposal. It requires high demands for any process using it, especially regarding the ventilation of the premises. The electrolyte

heated up considerably (up to 40 °C) when the current passed through it, which led to degradation of the electrolyte. This required cooling the bath intensively, as perchloric acid is explosive at elevated temperatures.

The third electrolyte used was a combination of tartaric acid ($C_4H_6O_6$), sodium bicarbonate ($NaHCO_3$), and water (H_2O). The mutual solubility of the components was first tested in a small amount. The preparation of the electrolyte entails two limitations: the solubility of soda in water (mostly 9.6 g/100 mL H_2O 20 °C) and the violent nature of the acid–base reaction. The amount of dissolved tartaric acid affects the solubility of sodium bicarbonate. The tests showed that the maximum solubility of soda in a mixture of acid and water was 9.3% by weight. Tartaric acid 5.5% by weight was chosen as the optimal ratio, and the remaining 85.2% by weight was water.

2.3. Experimental Planning

In the present research work, the electrolyte containing tartaric acid, sodium bicarbonate, and water was used. The experiments were performed by varying the different combinations of parameters using a full factorial design approach, as mentioned in Table 1, and for these experiments, the time duration was chosen to be 3 min. To study the effect of voltage and etched surface area on the passing current, the voltage was varied at five levels (4, 6, 8, 10, and 15 V) and the etched surface area was varied at nine levels. To study the effect of voltage on current density with electrode distance, the voltage was varied at 5 levels (4, 6, 8, 10, and 15 V) and the electrode distance was varied from 5 mm to 195 mm at increments of 10 mm (18 levels of electrode distance were used). The voltage was varied from 1 V to 20 V with step of 1 volt to study its effect on the current density. The effect of temperature on the current density was also studied by varying the temperature in the range of 26 °C to 38 °C with a step of 1 °C. The HVOF coating was removed from the different samples with different conditions: a fine condition with a lower voltage value (0 to 4 V), a productive condition (with a moderate voltage value of 5 to 10 V), and an intensive condition (higher value of voltage > 10V). In the intensive condition, it was observed whether the base material was affected or not. Further experiments were performed to remove the HVOF coating from the square cross-section prismatic bar using a single electrode and multi-electrodes. Further, the HVOF coating was removed from the components that were tab SB-002JI-5 TOOLOX-11 and hexagonal mandrel SB-00EA-1 160 TIS. The experimental process steps are mentioned in the following flow chart, as shown in Figure 3.

Table 1. The parameters varied during the experiments and their values.

Exp. Set	Voltage (Volt)	Etched Surface Area (cm^2)	Electrode Distance (mm)	Electrolyte Temperature (°C)
1.	4, 6, 8, 10, and 15	2.4, 4, 6, 8, 10, 12, 14, 16, and 18	45	31
2.		18	5 to 195 with increment of 10 mm	
3.	1 to 21 with increment of 1 volt		55	21
4.	8		55	26 to 38 with increment of 1 °C

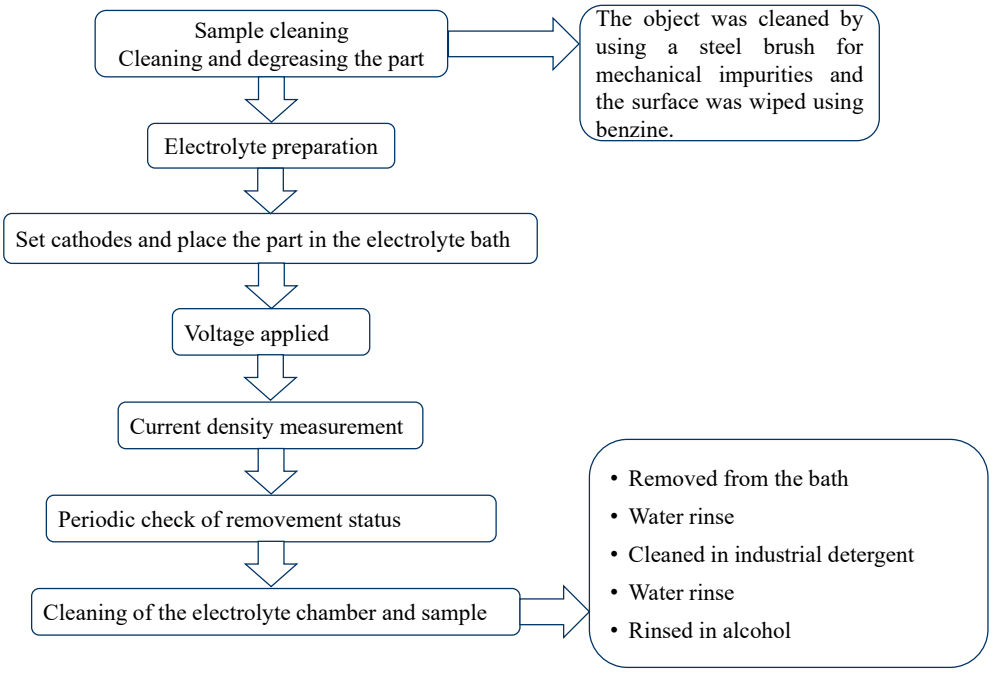

Figure 3. Flow chart for experimental process steps.

3. Results and Discussion

The experiments were performed on different samples. The effect of voltage on the dependency of the passing current with the etched surface area is shown in Table 2 and Figure 4. The effect of voltage on the current density with the electrode distance is mentioned in Table 3 and Figure 5. The effect of only voltage on the current density is shown in Table 4 and Figure 6. The effect of electrolyte temperature on the current density is mentioned in Table 5 and Figure 7. The study of removing the HVOF coating from the planar surface with different conditions was performed, and its results are shown in Figures 8–11. Experiments were also performed using a single electrode and multi-electrodes to remove the HVOF coating from the square cross-section prismatic bar, and those results are shown in Figures 12 and 13. The HVOF coating was also removed from the components, as shown in Figure 14.

3.1. Effect of Etched Surface Area on Current

A sample was used to measure the dependency of the passing current on the etching surface area. The dependency was measured for five levels of constant voltage: 4 V, 6 V, 8 V, 10 V, and 15 V. All other parameters were constant. The electrode distance was constant, which was 45 mm. The temperature was constant at 31 °C. All other surfaces were isolated by using insulation tape. The surface $S = b \times a$, where b is constant at 20 mm, was gradually revealed to the height of the test sample. After readjusting the voltage, the current was always allowed to stabilize for 3 min. The measured values of the passing current are shown in Table 2. As the etching area increases, the current increases (Figure 4). Larger values of the etched surface area provide lower resistance to the current flow; hence, higher values of current were observed. By knowing the amount of current and etched area surface, the upper limit for the parameters can be defined.

Table 2. Measured values of current for different values of etched surface area and voltage.

Etched Surface Area S (cm²)	Current I (A)				
	U = 4 V	U = 6 V	U = 8 V	U = 10 V	U = 15 V
2.4	0.56	1.1	1.6	2	3.1
4	0.8	1.5	2.1	2.87	4.15
6	1	1.9	2.7	3.5	5.3
8	1.15	2.2	3.2	4.15	6.3
10	1.3	2.4	3.5	4.55	7.1
12	1.4	2.7	3.9	5.15	8
14	1.6	2.9	4.3	5.7	8.8
16	1.7	3.15	4.6	6.1	9.7
18	1.8	3.4	4.85	6.3	10.2

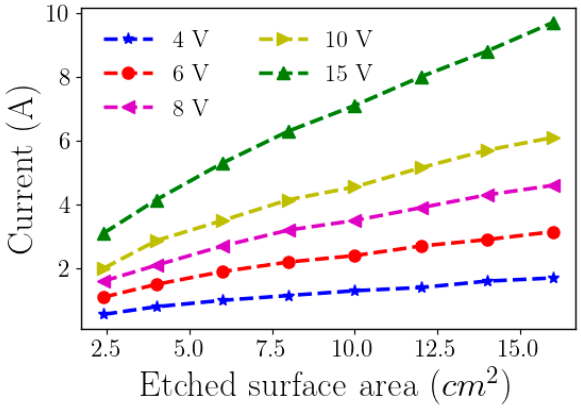

Figure 4. Variation in the current with etched surface area and voltage.

3.2. Effect of Electrode Distance on Current Density

A sample was used with an exposed area of 18 cm² to determine the dependency of the passing current on the distance between the electrodes. The other surfaces of the electrodes were masked with insulation tape. The dependency was measured for five constant voltage levels: 4 V, 6 V, 8 V, 10 V, and 15 V. The temperature was constant at 31 °C. The measured values of the current density are shown in Table 3. As the electrode distance increased, the current density decreased, as shown in Figure 5.

Table 3. Variation in current density with electrode distance and voltage.

Electrode Distance (mm)	Current Density J (A/dm²)				
	U = 4V	U = 6V	U = 8V	U = 10V	U = 15V
5	25.4	44.8	55.2	-	-
15	13.3	26.5	37.6	48.6	-
25	11.6	22.1	32.0	42.0	-
35	9.9	19.3	28.5	37.6	-
45	9.4	17.7	26.5	34.3	54.1
55	8.8	16.6	24.9	32.0	50.8
65	8.3	15.5	22.7	29.8	48.1
75	7.7	14.9	21.5	28.2	45.3
85	7.2	13.8	20.4	27.1	43.6
95	6.9	13.3	19.9	26.0	42.0
105	6.6	12.7	18.8	24.9	40.3

115	6.1	12.2	18.2	23.8	38.7
125	6.1	11.6	17.7	23.2	37.6
135	6.1	11.0	16.6	22.1	35.9
145	5.5	11.0	16.0	21.5	34.8
155	5.5	10.5	15.5	21.0	33.7
175	5.0	9.9	14.9	19.3	32.0
195	5.0	9.4	13.8	18.2	29.3

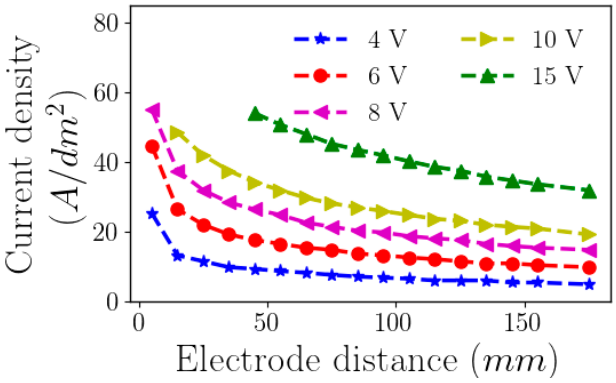

Figure 5. Variation in current density with electrode distance and voltage.

3.3. Effect of Voltage on Current Density

The voltage was varied from 1 to 20 V with a step of 1 V to study the dependency of the current density on it, as mentioned in Table 4. The experiments were performed with a constant electrode distance of 55 mm, a temperature of 21 °C, and an etched area of 18 cm^2. As the voltage increases, the current and current density increase. It is found that the variation is linear, and it is depicted in Figure 6. From this set of experiments, the value of voltage can be defined for safer operation by using the upper limit of current density (≈24 V), which did not etch the base materials during HVOF coating removal.

Table 4. Variation in current density with voltage.

U (volt)	I (A)	J (A/dm²)	U (volt)	I (A)	J (A/dm²)
1	0.1	0.6	11	4.8	26.5
2	0.3	1.7	12	5.3	29.3
3	0.7	3.9	13	5.8	32.0
4	1.2	6.6	14	6.3	34.8
5	1.7	9.4	15	6.8	37.6
6	2.3	12.7	16	7.4	40.9
7	2.8	15.5	17	7.9	43.6
8	3.2	17.7	18	8.5	47.0
9	3.8	21.0	19	9	49.7
10	4.3	23.8	20	9.5	52.5

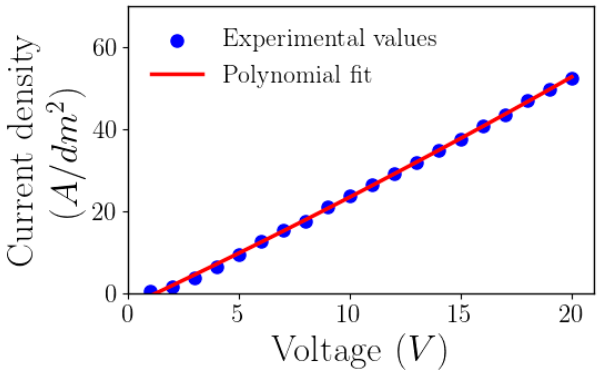

Figure 6. Variation in current density with voltage.

3.4. Effect of Electrolyte Temperature on Current Density

The dependency of the current density on the electrolyte temperature was carried out at constant voltage of 8 V, an etched area of 18 cm², and an electrode distance of 55 mm. As the temperature increases, according to theoretical assumptions, an increase in electrical conductivity of the electrolyte should also be evident. Thus, the increase in the current or current density is evident and is approximately linear, as shown in Figure 7. From a temperature of 34 °C, minor gas evolution begins to occur in the electrolyte. For practical use of this technology, the maximum etching temperature of 32 °C can be considered.

Table 5. Variation in current density with electrolyte temperature.

T (°C)	I (A)	J (A/dm²)	T (°C)	I (A)	J (A/dm²)
26	3.6	19.9	**33**	4.3	23.8
27	3.6	19.9	**34**	4.4	24.3
28	3.7	20.4	**35**	4.5	24.9
29	3.8	21.0	**36**	4.6	25.4
30	3.9	21.5	**37**	4.6	25.4
31	4.2	23.2	**38**	4.7	26.0
32	4.2	23.2			

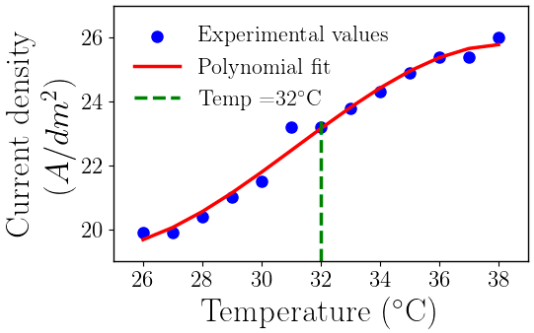

Figure 7. Variation in current density with temperature.

3.5. HVOF Coating Removal with Different Combinations of Process Parameters

After investigating the dependency of current density on the etched surface area, electrode distance, voltage, and electrolyte temperature, further experiments were conducted to remove the HVOF coating under varying conditions: (i) fine, using lower

voltage; (ii) productive, with moderate voltage; and (iii) intensive, with significantly higher voltage. The impact on the base material and the selection of parameters for steel corrosion protection were also evaluated.

Sample 2 was subjected to further dissolution with the following parameters: voltage at 6 V, electrolyte temperature at 26 to 28 °C, and electrode distance as 55 mm. After about 4 h, the sample started to show light edges with the coating removed. In the middle of the sample, the coating remains for removal (Figure 8a). In this state, the lower half of the sample was isolated with tape to prevent further dissolution and to make a metallographic cut with a target. The lower part of the sample isolated in this way is labeled 2A. The transition from the edge to the center is shown in Figure 8b. Metallographically, it was found that while the coating was completely removed at the edges (Figure 8c), there was still almost 0.1 mm of it in the center of the coating target (Figure 8d). The rest of the coating was already damaged by etching. The area of the back side of sample 2A was not exposed to the electrolyte, but 2B shows a very small amount of etching, as depicted in Figure 8e.

After masking the lower half of the sample, the upper half of 2B was dissolved under the following conditions: voltage at 6 V; electrolyte temperature at 26 to 28 °C; and electrode distance at 55 mm. To determine the reaction of the current to the base material, after a while, the upper half was also unmasked on the sides and the back-milled side of the sample. The unmasking resulted in an increase in the current from 1.4 A to 2.0 A. After another three hours of dissolution, the coating was completely removed (Figure 8f). Sample 2B on its reverse side showed minor corrosion at the edges. The corrosion attack was manifested by local graying and small corrosion pits on the surface. However, the traces of milling did not disappear, and it can be safely assumed that a small attack would not affect the dimensions of the part. Small corrosion pits (pitting) are more susceptible to subsequent atmospheric corrosion (Figure 8g).

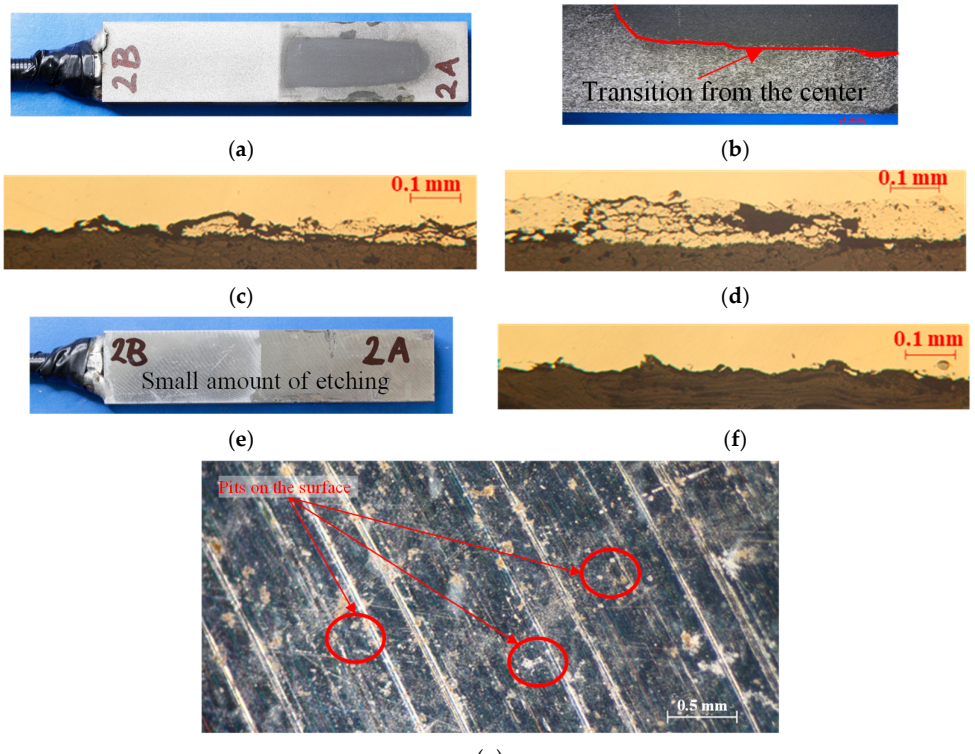

Figure 8. HVOF coating removal from sample 2: (**a**) lower half is masked, (**b**) transition from the edge to the center, (**c**) sample 2A (left), the edge of the sample, on the right, the transition to the

center of the sample, (**d**) sample 2A coating at the center, (**e**) sample 2B with minor etching, (**f**) complete removal of the coating, and (**g**) corrosion on sample 2B.

3.5.1. Fine Conditions Test

Sample number 3 was tested under mild conditions (lower value of voltage) that should eliminate the attack on the base material. The inter-electrode distance was chosen to be 85 mm. The conductivity of the electrolyte was around 100 mS, with a temperature range of 22 to 24 °C. The etching area was 18.1 cm^2. No surfaces on the sample were covered. The voltage was set as 3 V on the source. The passing current stabilized at a value of 0.7 A, which corresponds to the current density of 3.8 A/dm^2. After 16 hours of continuous operation, the etching was stopped. No change in coating thickness was observed. The coating was uniform over the entire area. It was apparently disturbed in some way, as it was intensively lubricated and had a black layer of chemical reaction products on it, which apparently could not be removed from the surface due to the reduced production of gas bubbles. The base material did not show any point of attack.

3.5.2. Test of Productive Conditions

After the fine test, the voltage on sample no. 3 was increased to 6 V. The current stabilized at a value of 2.3 A, which corresponds to a current density of 12.7 A/dm^2. After 5.5 h, the coating was completely removed (Figure 9). The attack of the base material was lower than in the case of sample 2B.

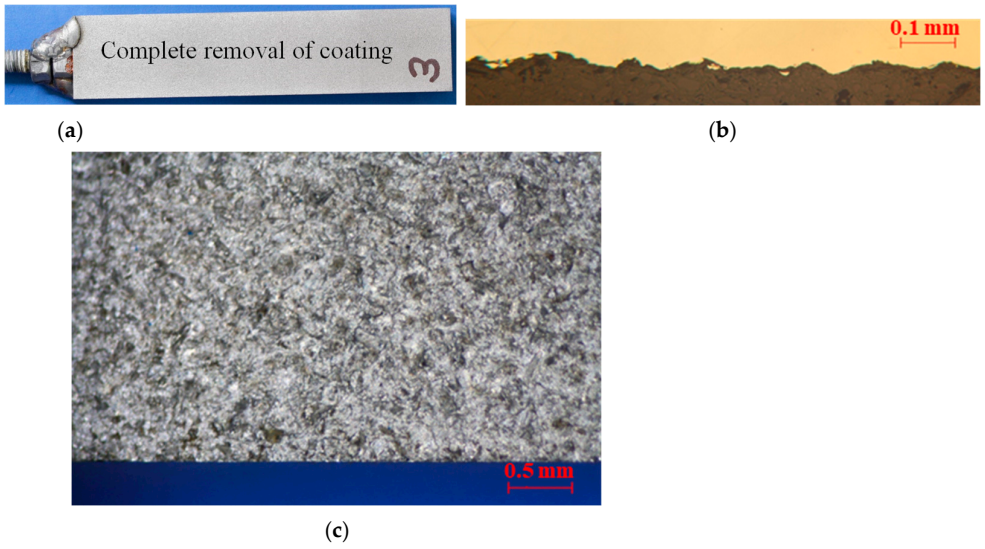

(**a**) (**b**)

(**c**)

Figure 9. Removal of coating from sample 3 with productive conditions: (**a**) top view, (**b**) side view, and (**c**) macro-image of the surface without coating residues.

3.5.3. Test on the Effect of Intensive Conditions on the Base Material

After removing the coating from sample 3, the back side of the sample was subjected to intensive conditions to determine the impact on the base material. The inter-electrode distance was reduced to 35 mm to make the dissolution process more intensive. Due to intensive conditions, the electrolyte temperature was increased. The voltage was set at 12 V and the corresponding current was settled at 9.2 A and increased with increasing temperature until it reached the limit of 10.2 A by the source. In order not to damage the source, the voltage had to be reduced during the test. The test was completed after 2 h at a temperature of 50 °C, voltage of 10 V, and corresponding current of 10 A. The surface

was damaged. Local spot corrosion is noticeable, especially on the milled side, as shown in Figure 10.

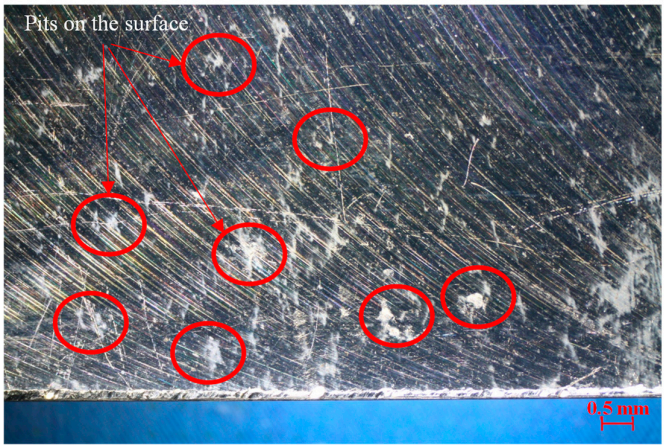

Figure 10. Pitting on the surface of coating removal.

Overall, the three tests demonstrate a progressive increase in the severity of the conditions applied, from mild etching that leaves the base material unaffected (fine conditions test) to more aggressive etching that removes the coating without severe damage to the base (productive conditions rest), and finally, to intensive conditions that cause visible damage to the base material but with limited depth or density of corrosion (intensive conditions test).

3.5.4. Selection of a Key Parameter for the Corrosion Protection of Steel

The lower half of the sample (45 mm) was covered with insulating tape and labeled 4A. The sample was corroded as shown in Figure 11a. A voltage of 15 V was set on the source. A current of 5.3 A passed through the electrolyte. The electrode distance was chosen to be 135 mm. Due to the increased voltage, the electrolyte heated up, and the current increased to 6.4 A within 60 min. After 60 min, the sample was inspected. There was clear graying and etching along the edges on the back milled side (Figure 11b). The coating had a drop in thickness but remained intact. The upper half was marked 4B. For the next 180 min, the sample was exposed to the opposite combination of conditions. A minimum electrode distance of 5 mm was chosen. The source worked in the reduced voltage mode at 4.5 V/3.5 A. After 180 min, there was no significant deterioration of the base material. Traces of milling remained visible. The surface was no longer etched to gray, only the dimples had been accentuated. Local differences in the dissolution rate occurred on the injection side. In the center of the surface and at the edges, a coating with a thickness of 0.25 mm remained, while in some parts the coating had already been completely removed. With a longer etching time, the coating would probably be completely removed.

It follows from the above that the attack of the base material is dependent to a greater extent on the voltage than on the electrode distance. Therefore, it is more appropriate to achieve the required current densities precisely by reducing the electrode distance. The reduced electrode distance entails higher demands on the negative of the cathode when applied to shaped parts. In the final test on sample 4, the top half of the 4B etched in the previous step was covered. The lower half of sample 4A was exposed. The etching parameters of the lower half of sample 4 were as follows: a voltage of 4.5 V; a current of 1.6 A; and an electrode distance of 55 mm. The coating was completely removed after 10 h. Attack on the base material was negligible.

From the study of the dependency of current density on the etched area, voltage, electrode distance, and electrolyte temperature, it can be seen that the current density decreases with the electrode distance and etched area. In the case of parts where corrosion of the base material is unacceptable, a voltage on the source in the range of 4 to 6 V can be recommended. Faster material removal and higher current densities should be achieved with a smaller electrode distance (10 to 35 mm). In the case of parts that have a coating on all surfaces, a voltage in the range of 6 to 12 V can be recommended. At higher voltages, the electrode distance can be increased, and the necessary current densities can be maintained. A larger electrode distance places lower demands on the shape of the cathode for shaped elements. At higher voltages, there is more gas production at the anode, which promotes electrolyte mixing, resulting in pure metallic gray surfaces after blasting, with no coating residue.

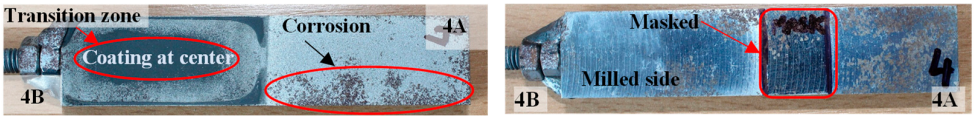

(**a**) (**b**)

Figure 11. Sample 4 with coating removal: (**a**) corrosion and (**b**) milled side, masked part in the middle, negligible attack area 4A.

3.6. Application of Technology to Shaped Parts

The HVOF coating was removed on the different simulated shaped parts and the process capabilities were studied.

3.6.1. HVOF Coating Removal from a Shaped Part Using a Single Electrode

Before the delivery of the shaped parts, the ability to etch the shaped parts was tested on a system of four samples assembled into a rectangle, as shown in Figure 12. The lower half of the sample was masked all around. The aim was to test whether surface passivation would occur if the cathode area was smaller than the coating area. In general, it is recommended to choose a cathode area at least 2.5 times the anode area. Furthermore, it was necessary to obtain information about the dissolving ability of the surface that is not facing the cathode, i.e., samples 6, 7, and 8.

A new electrolyte was prepared for the test. The voltage was chosen as 6 V, the corresponding current was 2.2 A, and the electrodes were at a distance of 50 mm. The electrolyte bath was checked after 12 hours. On sample no. 5, the coating was completely removed at the edges, and a small coating target of practically unmeasurable thickness remained in the middle. Specimen nos. 6 and 7 had slightly lightened edges, but the coating was solid over almost the entire surface. Specimen no. 8 facing away from the cathode showed thinning of the coating but remained completely intact. After another 6 h of etching, the coating from specimen no. 5 was completely removed and showed a clean metallic gray surface. Specimen nos. 6, 7, and 8 also had the coating removed in the entire area; however, the surface had a darker impression, and the small differences were lost. The total coating removal time in this configuration was 18 hours.

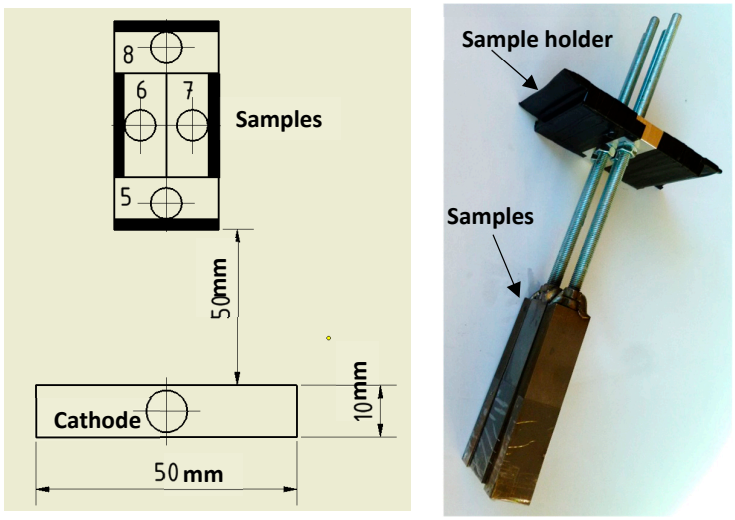

Figure 12. HVOF coating removal using single cathode: (**a**) sample assembly schematic; (**b**) assembled samples for shape simulation.

3.6.2. HVOF Coating Removal from a Shaped Part Using Four Electrodes

The configuration was slightly changed to four electrodes, as shown in Figure 13a. The top half of the sample was masked. The electrode distance was chosen to be 35 mm for each specimen. The voltage was chosen to be 6 V, and the current was 3.9 A flowing through the electrolyte. Due to the passage of electric current, a noticeable increase in temperature and the amount of dissolved metal was observed, and the conductivity of the electrolyte increased during etching; at the end of the experiment, a current of 6.2 A flowed through the electrolyte. The etching on the specimen was uniform, and the coating was completely removed after 10 h.

A damaged SB-002JI-5 TOOLOX-11 tab was supplied as a representative of plate-type flat parts, as shown in Figures 14a and 14b. A voltage of 5.3 V was set on the source, which corresponded to a current of 9.7 A. The current density related to the coating area was 5.4 A/dm^2. The coating was completely removed after 22 h. The etching of the SB-00EA-1 160 TIS mandrel, as shown in Figure 14c, was conducted in one step due to the smaller etched area. The immersion depth in the electrolyte was 118 mm. The mandrel was surrounded by six electrodes arranged approximately in a hexagon so that the same distance between the surface of the anode and the cathode was maintained. A voltage of 6 V was set on the source, and a current of 10 A flowed through the electrolyte. After 7 h, the coating was completely removed on almost the entire surface.

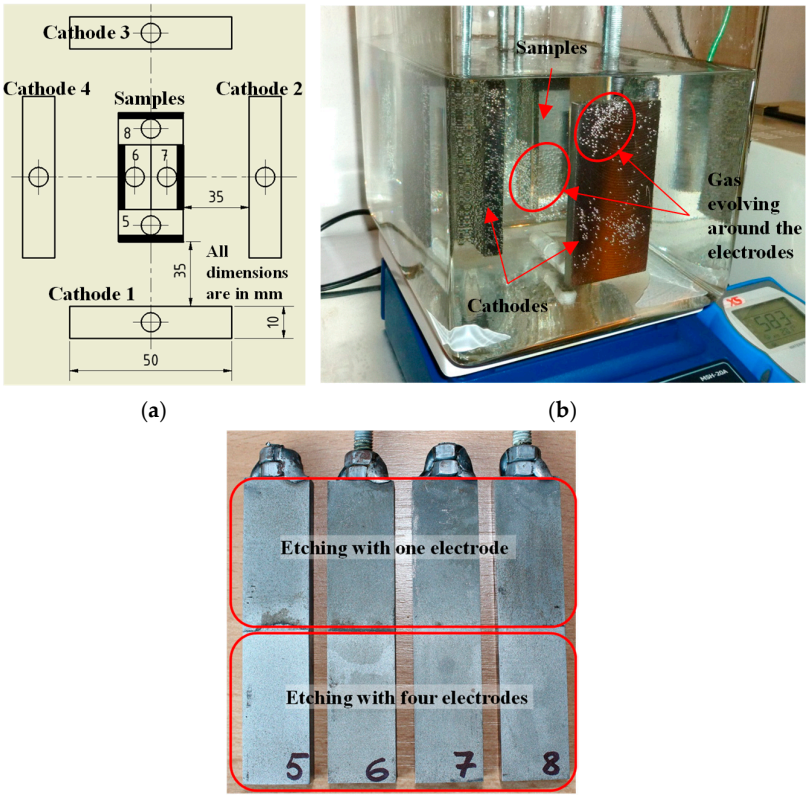

Figure 13. HVOF coating removal using multi-electrode: (**a**) assembly of samples; (**b**) electrode suspension position in the bath; and (**c**) appearance of samples after shape simulation: top etched with one cathode, bottom etched with four cathodes.

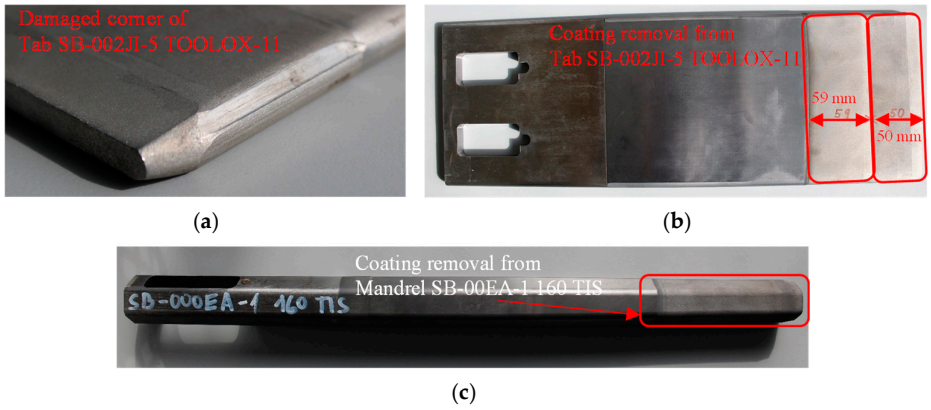

Figure 14. (**a**) Tab SB-002JI-5 TOOLOX-11, (**b**) tab SB-002JI-5 TOOLOX-11 with two-stage etched coating, and (**c**) mandrel SB-00EA-1 160 TIS with coating removal.

4. Conclusions

The objective of this work was to study the effect of various parameters, which were voltage, surface area, electrode distance, and electrolyte temperature, on current density for the purpose of HVOF coating removal. The electrolyte used in the experiments was a combination of tartaric acid, sodium bicarbonate, and water. A feasibility study confirmed the effective removal of the WCCoCr 86/10/4 HVOF coating. The major achievements of the present research work are as follows:

- HVOF coating removal is possible by using a non-contact process, electrolytic dissolution, without damaging the integrity of the base materials.
- The following process parameters are recommended for removing the coating completely without etching the base material with duration of 10 h: a voltage of 4.5 V; an electrolyte temperature of 26–28 °C; and an electrode distance of 55 mm,.
- The experiments measured the current dependency across different etched surface areas while keeping the temperature and electrode distance constant. It was found that the current increased with the surface area, but the current density decreased.
- The current density decreased with electrode distance, establishing an inverse relationship between them.
- A direct relationship was found between the voltage and current density at a fixed temperature, electrode distance, and etched area. The results indicated a linear increase in current density with voltage.
- Higher temperatures resulted in increased current density, though a maximum threshold (32 °C) was suggested to prevent significant gas evolution and electrolyte degradation.
- From the experiments for different test conditions, it was found that in the fine and productive conditions with low and moderate values of voltage, the HVOF coating was removed successfully without etching the base material, as compared to the intensive condition with a higher value of voltage.
- The experiments with a single cathode and four cathodes showed that multiple cathodes enhanced the uniformity and reduced the coating removal time.
- The real-world application of the electrolytic dissolution process was tested on actual components, TOOLOX-11 tab and hexagonal mandrel, proving effective at achieving the desired coating removal.
- The presented method was used to remove the HVOF coating with a certain range and combination of process parameters and taking more time for successful removal without affecting the base material. It is applicable only for the overhaul of the components, for those that do not require frequent recoating, because it is time-consuming process. Other than the above limitation, the electrolytic dissolution is applicable only for conductive materials.
- The present study can be extended to other electrolytes to find if lower values of the input parameter voltage, electrode distance, and electrolyte temperature can give the same effective removal of coating in terms of utilizing less energy input.

Author Contributions: Conceptualization: Z.P., M.S., J.K., L.B., S.P., and V.R.; methodology: Z.P., M.S., J.K., L.B., S.P., and V.R.; validation: Z.P., M.S., J.K., and L.B.; investigation: Z.P., M.S., J.K., and L.B.; writing—original draft preparation: V.R., S.P., and Z.P.; writing—review and editing: V.R., S.P., and L.B.; supervision: S.P. and L.B.; project administration: L.B.; funding acquisition: S.P. and L.B. All authors have read and agreed to the published version of the manuscript.

Funding: This work was co-funded by the European Union and the state budget of the Czech Republic under the project LasApp CZ.02.01.01/00/22_008/0004573. This work was also supported by the infrastructure of the Centre of Advanced Aerospace Technology, Project No. CZ.02.1.01/0.0/0.0/16_019/0000826 and project SGS22/158/OHK2/3 T/12, Faculty of Mechanical Engineering, Czech Technical University in Prague.

Data Availability Statement: All the data are presented in the manuscript.

Conflicts of Interest: The authors declare no conflicts of interest.

References

1. Lee, H.-B.; Lin, T.-J.; Lee, C.-Y. Corrosion of high-velocity-oxygen-fuel (HVOF) sprayed non-crystalline alloy coating in marine environment. *Surf. Coat. Technol.* **2021**, *409*, 126896. https://doi.org/10.1016/j.surfcoat.2021.126896.
2. Wu, M.; Pan, L.; Duan, H.; Wan, C.; Yang, T.; Gao, M.; Yu, S. Study on Wear Resistance and Corrosion Resistance of HVOF Surface Coating Refabricate for Hydraulic Support Column. *Coatings* **2021**, *11*, 1457. https://doi.org/10.3390/coatings11121457.
3. Santana, Y.Y.; La Barbera-Sosa, J.G.; Bencomo, A.; Lesage, J.; Chicot, D.; Bemporad, E.; Puchi-Cabrera, E.S.; Staia, M.H. Influence of mechanical properties of tungsten carbide–cobalt thermal coating coatings on their solid particle erosion behaviour. *Surf. Eng.* **2012**, *28*, 237–243. https://doi.org/10.1179/1743294411y.0000000016.
4. Vats, A.; Kumar, A.; Patnaik, A.; Meena, M.L. Influence of deposition parameters on Tribological Performance of HVOF Coating: A review. *IOP Conf. Ser. Mater. Sci. Eng.* **2021**, *1017*, 012015. https://doi.org/10.1088/1757-899X/1017/1/012015.
5. Javed, M.A.; Ang, A.S.M.; Bhadra, C.M.; Piola, R.; Neil, W.C.; Berndt, C.C.; Leigh, M.; Howse, H.; Wade, S.A. Corrosion and mechanical performance of HVOF WC-based coatings with alloyed nickel binder for use in marine hydraulic applications. *Surf. Coat. Technol.* **2021**, *418*, 127239. https://doi.org/10.1016/j.surfcoat.2021.127239.
6. Singh, V.; Kumar, V.; Bansal, A.; Singla, A.K.; Verma, R. Corrosion–Cavitation Erosion Improvement of Marine Steel by High-Velocity Oxy-fuel-Sprayed Vanadium Carbide Coatings and Polytetrafluorethylene Topcoat. *J. Mater. Eng. Perform.* **2024**. https://doi.org/10.1007/s11665-024-09711-0.
7. Ma, X.; Ruggiero, P.; Bhattacharya, R.; Rai, A.K. Optimization of HVOF-Applied Erosion-Resistant Coatings for Large Compressor and Fan Airfoils in STOVL Aircrafts. *J. Therm. Coat. Technol.* **2024**, *33*, 367–380. https://doi.org/10.1007/s11666-023-01681-4.
8. Mora, J.; García, P.; Muelas, R.; Agüero, A. Hard Quasicrystalline Coatings Deposited by HVOF Thermal Coating to Reduce Ice Accretion in Aero-Structures Components. *Coatings* **2020**, *10*, 290. https://doi.org/10.3390/coatings10030290.
9. Li, N.; Wang, Q.; Dong, F.; Liu, X.; Han, P.; Han, Y. Research Progress of Coating Preparation on Light Alloys in Aviation Field: A Review. *Materials* **2022**, *15*, 8535. https://doi.org/10.3390/ma15238535.
10. Farokhian, G.; Salehnasab, B.; Zat Ajam, H.; Nahidi, H. Influence of WC–20Co–1Ni coating by HVOF on lifespan of the downhole drilling motors. *Surf. Eng.* **2018**, *34*, 771–782. https://doi.org/10.1080/02670844.2017.1278643.
11. Kılıç, H.; Mısırlı, C. Investigation of tribological behavior of 20NiCrBSi-WC12Co coated brake disc by HVOF method. *Mater. Res. Express* **2020**, *7*, 016560. https://doi.org/10.1088/2053-1591/ab61be.
12. Usmani, S.; Sampath, S.; Houck, D.L.; Lee, D. Effect of Carbide Grain Size on the Sliding and Abrasive Wear Behavior of Thermally sprayed WC-Co Coatings. *Tribol. Trans.* **1997**, *40*, 470–478. https://doi.org/10.1080/10402009708983682.
13. Nahvi, S.M.; Jafari, M. Microstructural and mechanical properties of advanced HVOF-sprayed WC-based cermet coatings. *Surf. Coat. Technol.* **2016**, *286*, 95–102. https://doi.org/10.1016/j.surfcoat.2015.12.016.
14. Sahraoui, T.; Fenineche, N.-E.; Montavon, G.; Coddet, C. Alternative to chromium: Characteristics and wear behavior of HVOF coatings for gas turbine shafts repair (heavy-duty). *J. Mater. Process. Technol.* **2004**, *152*, 43–55. https://doi.org/10.1016/j.jmatprotec.2004.02.061.
15. Nascimento, M.P.; Souza, R.C.; Miguel, I.M.; Pigatin, W.L.; Voorwald, H.J.C. Effects of tungsten carbide thermal spray coating by HP/HVOF and hard chromium electroplating on AISI 4340 high strength steel. *Surf. Coat. Technol.* **2001**, *138*, 113–124. https://doi.org/10.1016/S0257-8972(00)01148-8.
16. Hazra, S.; Sabiruddin, K.; Bandyopadhyay, P.P. Plasma and HVOF sprayed WC–Co coatings as hard chrome replacement solution. *Surf. Eng.* **2012**, *28*, 37–43. https://doi.org/10.1179/1743294410Y.0000000009.
17. Ruusuvuori, K.; Lahdenpera, K.; Oksa, M.; Turunen, E.; Kauppila, J.; van Wonderen, M. Controlled HVOF hard coating removal method. In Proceedings of the 2005 WJTA American Waterjet Conference, Paper 5B-2, Houston, TX, USA, 21–23 August 2005.
18. Bolelli, G.; Lusvarghi, L.; Barletta, M. HVOF-sprayed WC–CoCr coatings on Al alloy: Effect of the coating thickness on the tribological properties. *Wear* **2009**, *267*, 944–953. https://doi.org/10.1016/j.wear.2008.12.066.

19. Sapate, S.G.; Tangselwar, N.; Paul, S.N.; Rathod, R.C.; Mehar, S.; Gowtam, D.S.; Roy, M. Effect of Coating Thickness on the Slurry Erosion Resistance of HVOF-sprayed WC-10Co-4Cr Coatings. *J. Therm. Coat. Technol.* **2021**, *30*, 1365–1379. https://doi.org/10.1007/s11666-021-01190-2.
20. Globisch, S.; Friedrich, M.; Heidemann, N.; Döpper, F. Tool Concept for a Solid Carbide End Mill for Roughing and Finishing of the Tool Steel Toolox 44. *J. Manuf. Mater. Process.* **2024**, *8*, 170. https://doi.org/10.3390/jmmp8040170.